Ice-rafted dropstones in 'post-glacial' Cryogenian cap carbonates

Le Heron, Daniel Paul; Busfield, Marie; Kettler, Christoph

Published in:
Geology

DOI:
10.1130/G48208.1

Publication date:
2021

Citation for published version (APA):
Le Heron, D. P., Busfield, M., & Kettler, C. (2021). Ice-rafted dropstones in 'post-glacial' Cryogenian cap carbonates. *Geology*, *49*(3), 263-267. https://doi.org/10.1130/G48208.1

Ice-rafted dropstones in 'post-glacial' Cryogenian cap carbonates

Le Heron, D.P[1]. Busfield, M.E[2]., Kettler, C[1].

[1]*Department of Geodynamics and Sedimentology, University of Vienna, Althanstrasse 14, 1090 Vienna, AUSTRIA.* daniel.le-heron@univie.ac.at

[2]*Department of Geography and Earth Sciences, Aberystwyth University, Llandinam Building, Penglais Campus, Aberystwyth, SY23 3DB.*

Abstract

Dropstones of ice-rafted origin are typically cited as key cold-climate evidence in Cryogenian strata, and according to conventional wisdom should not occur in post-glacial, warm water carbonates. In Namibia, the Chuos Formation (early Cryogenian) contains abundant dropstone-bearing intervals and striated clasts. It is capped by the Rasthof Formation, comprising laminites in its lower portion, and microbial carbonates above. These laminites are locally found to contain pebble- and granule-sized lonestones in abundance. At Omutirapo (Fig. 1), metre-thick floatstone beds occur at the flanks of a Chuos palaeovalley, and are readily interpreted as mass flow deposits. At Rasthof Farm, however, the clasts warp, deflect and penetrate hundreds of carbonate laminations at both the outcrop and thin section scale. We propose that these are dropstones, and envisage an ice-rafting mechanism. Evidence for vestigial glaciation concomitant with cap carbonate deposition thus merits a reappraisal of the depositional conditions of cap carbonates and their palaeoclimatic significance.

INTRODUCTION

The glacial affinity of diamictites and lonestone-bearing sedimentary rocks in the Cryogenian record is compelling (Hoffman and Halverson, 2008; Le Heron et al., 2013; Busfield et al., 2013; Bechstädt et al., 2018; Hoffman et al., 2017). By comparison, all models for cap carbonates envisage a postglacial origin (Yu et al., 2020). These are commonly thought to record a high alkalinity flux and sudden oceanic oxidation following rapid meltback of global ice cover (e.g. Shields, 2005; Hoffman et al., 1998), possibly representing stratigraphic condensation during globally synchronous deglaciation (Rooney et al., 2020).

In Namibia, the Chuos Formation (of glacial origin) is overlain by the Rasthof Formation (cap carbonate) that is interpreted to record the abrupt change to a significantly warmer greenhouse climate (Hoffmann and Prave, 2004; Hoffman et al., 2017). Here, we compare evidence from two outcrops of the Rasthof Formation, both of which contain clast-rich intervals sandwiched between clast-free dololaminites. One of these (from Omutirapo) represents a mass flow deposit; another from Rasthof Farm, with lonestones puncturing delicate laminites, is interpreted as a cluster of ice-rafted dropstones. We posit that the dropstones require the presence of floating ice to explain their occurrence in the purportedly warm water cap carbonates, with implications for Cryogenian deglaciation on a global-scale.

GEOLOGIC BACKGROUND AND STUDY AREA

Cryogenian glacial (diamictite-bearing siliciclastics) and postglacial (cap carbonate) rocks crop out along the southern and western flanks of the Owambo Basin, northern Namibia (**Fig. 1**) (Miller, 2008). Diamictite-bearing rocks of the Chuos Formation sit unconformably upon the Nosib Sandstone Group, with the Rasthof Formation in turn lying above (**Fig. 2**). At Omutirapo (**Fig. 1**), the Chuos Formation attains >400 m thickness in a glacial palaeovalley and is interbedded with lonestone-bearing and lonestone-free intervals (Le Heron et al., 2013), which record glacial to interglacial transitions. Subsequent work (Hoffman et al., 2017) at Omutirapo has confirmed earlier interpretations of a major subglacial topography. Detailed micromorphological studies have distinguished glacial from non-glacial modes of emplacement for diamictites by comparison to modern and Quaternary subglacial diamicts (Busfield et al., 2013; Busfield and Le Heron, 2018). The role of mass flow sedimentation in the Chuos (Eyles and Januszczcak, 2007) remains undisputed although the evidence for glacial processes also remains strong (Le Heron et al., 2013). The Rasthof Formation is a cap carbonate that directly overlies the Chuos (Hoffman and Halverson, 2008), and which comprises a micritic dololaminite member overlain by a microbial member comprising stromatolites and thrombolites (Le Ber et al., 2013). A marine origin is suggested on account of the agglutinated foraminifera that it contains (e.g. Bosak et al., 2012, Dalton et al., 2013). In palaeogeographic terms, the study areas represent rocks deposited on a stable marine platform (the Northern Platform: Hoffman et al., 2008). A second diamictite-rich interval, the Ghaub Formation, occurs at a higher level in the stratigraphy. Bechstädt et al. (2018) noted that a non-glacial origin for the diamictites “is questioned by possible dropstones that occur in beds transitional to and, rarely, also within the cap carbonates”. Thus, the occurrence of “possible dropstones” in other cap carbonate successions, such as the Rasthof Formation, merits reappraisal.

DESCRIPTION

We studied two exposures in which outsized clasts (lonestones) occur within the Rasthof Formation. These are (i) the Omutirapo succession and (ii) at Rasthof Farm (**Fig. 1**). In both cases, the uppermost part of the Chuos Formation comprises massive diamictite, and the basal part of the Rasthof Formation comprises delicately laminated dolomicrites which sit in sharp contact upon the underlying glacial deposits (**Fig. 2**, **Fig. 3** A). Lonestone-bearing carbonates (granule to pebble-sized clasts embedded in a micrite matrix) are common. Two subfacies are recognised. First, at

Omutirapo, ca. 10 m thick laminated dolomicrites contain a 1 m thick floatstone bed (**Fig. 3** B) which passes along strike over ca. 100 m into normally-graded packstones (**Fig. 3** C). The floatstone interval contains sub-rounded to rounded, equant, dolostone clasts (**Fig. 3** D), with highly attenuated, bedding parallel clasts in the basal 10 cm (**Fig. 3** E). Second, at Rasthof Farm (**Fig. 2**, **Fig. 4** A), a 50 cm interval of mm-thick laminated dolomicrites, contains abundant granule to small pebble-sized lonestones up to 2 cm diameter (**Fig. 4** B). At the outcrop / hand-specimen scale, lonestone-bearing laminations are sandwiched between dololaminites in which outsized clasts are absent (**Fig. 4** B). Most lonestones exhibit both impact structures beneath them, and draping lamination (undisturbed dololaminae) overlie them (Fig. 4 B-E). Small, lens-like clast clusters (**Fig. 4** B) also occur. Clasts include abundant dolomite granules, quartz (**Fig. 4** C, D) and lithic fragments (**Fig. 4** E). At the thin-section scale, the occurrence of lonestones at multiple levels is demonstrable (**Fig. 4** F). Both irregular clast clusters and individual clasts, including 1 cm diameter intraclasts (**Fig. 4** F) punctuate mm-thick laminae, and are draped by undisturbed dolomicrite laminae. A full 3D model of the sampled interval is available as Supplementary Material.

INTERPRETATION

The lonestone-bearing carbonates at Omutirapo and Rasthof Farm are attributable to two different processes. At Omutirapo, the absence of laminations (**Fig. 3** C) is compatible with gravitational emplacement as previously suggested (Hoffman et al., 2008), in which attenuated basal clasts (**Fig. 3** E) probably record shearing at the base of a mass flow. Cap carbonate collapse facies are now widely recognised elsewhere (e.g. Creveling et al., 2016), and at Omutirapo, a non-glacial mechanism is envisaged. At Rasthof Farm, by contrast, we propose that the lonestone-bearing laminite interval records ice-rafted deposition. Puncturing of mm-thick laminae by granule- to pebble-sized clasts testifies to their emplacement from above, representing settling through a water column. They are thus interpreted as ice rafted debris (IRD). Their presence within finely laminated dolomicrites is thus hydrodynamically paradoxical (Bennett et al., 1996). The clast clusters are interpreted as sedimentary pellets (Tomkins et al., 2008). Although there is a tradition of recognising “outrunner clasts” from debris flows where an ice-rafted mechanism is not appealing (Kennedy and Eyles, 2020), this process cannot explain granule and pebble-sized clasts in laminated dolomicrites. This is because although hydroplaning beneath much larger-scale “outrunner blocks” e.g. in olistostromes is possible, the mechanics do not work at the finer-grained end of the Udden-Wentworth scale (Peakall et al., 2020). Furthermore, the absence in the study interval of wave-ripple (Lamb et al., 2012) or hummocky cross stratification structures locally seen elsewhere in the Rasthof (Le Ber et al., 2013) rules out a tractive origin for the lonestones.

In the Paleozoic record, kelp or fucid rafting explains some dropstones (Zalasiewicz and Taylor, 2001). Time-calibrated phylogeny of green seaweeds (Del Cortona et al., 2020) suggests that their ancestors may have been present in the Cryogenian. Yet rafting by seaweeds torn from the shore (e.g. by storms) is incompatible with interpretations of the dololaminites in the Rasthof. These, like other dololaminites in cap carbonates record pelagic precipitation, irrespective whether this is chemically or biogenically mediated (c.f. Hoffman and Schrag, 2002; Shields, 2005; Kennedy and Christie-Blick, 2011). Thus, given the absence of other mechanisms which could adequately explain the emplacement of dropstones (seaweed rafting, driftwood rafting, gastroliths: Bennett et al., 1996) we find that they indicate floating ice during Rasthof deposition. This finding is significant, because “no convincing dropstone has been confirmed from cap dolostone units anywhere in the world” (Shields, 2005, p.301).

DISCUSSION AND CONCLUSIONS

Two scenarios for the IRD emerge: (i) as glacial sediment advected into open water by either an ice shelf or calving icebergs, or alternatively (ii) through melting sea ice. Additional physical evidence for iceberg activity (e.g. iceberg keel plough marks: Vesely and Assine, 2014) has never been found in the Cryogenian record. Analysis of cores through Heinrich layers in the polar North Atlantic reveals IRD are up to small pebble-size and concentrated along discrete horizons and linked to major iceberg calving events (Hodell et al., 2017). In contrast, the Rasthof Farm IRD are scattered over hundreds of laminations, suggesting multiple ice melting events.

The development of floating sea ice or ice shelves must therefore be considered. Pebble-sized clasts, deposited through shorefast ice in large lakes can also occur (Oviatt, 2018), and thus clast size is of little use in inferring the nature of the floating ice source. In modern high latitude settings such as the Antarctic Peninsula, eolian sediment is transported over seasonal sea ice during the winter months. Upon melting, sand particles are released into the open marine environment (Chewings et al., 2014). These processes result in dispersed sand and granule sized particles in laminites. The same processes explain a significant component of open marine sedimentation in the Arctic, whereby the advection of sand and coarser material over developing frazil ice, together with mud-grade sediment, is also well established (Kempena et al., 1989). Basal meltout beneath floating ice shelves would also account for IRD, in which the sedimentary pellets may be interpreted as meltout of till (Tomkins et al., 2008).

In terms of the host strata, dololaminites above Cryogenian glacial successions are classically considered to result from a massive alkalinity flux stimulated through either carbon dioxide (Hoffman et al., 1998) or methane (Kennedy et al., 2001) outgassing, through continental weathering of freshly exposed continental material (Hoffman et al., 2017), or by the precipitation of whitings during algal blooms within a low salinity meltwater plume (Shields, 2005). Some have proposed that tillite weathering might account for cap carbonate deposition (Fabre and Berger, 2012). This latter mechanism has parallels with the proposals of Fairchild et al. (1989) who suggested that “massive recrystallization of glacially transported carbonate is proposed as a geologically significant process”. All of these mechanisms require that the dololaminites represent pelagic materials deposited postglacially in an ameliorated climate. Assuming a global ice cover, energy-balance calculations have suggested a global mean surface temperature swing from -50 C during a glaciation to approximately +40 C during interglacial (cap carbonate) times (Hoffman and Schrag, 2002, their Fig. 7). Such high temperatures are difficult to reconcile with the scattered occurrence of the dropstones across hundreds of laminae: a sudden melting mechanism would instead be expected to release an iceberg armada and intense concentration of dropstones across a single stratigraphic interval. These textures are not observed at Rasthof Farm.

As precedents, dropstones are now recognised to occur in other Neoproterozoic successions where according to conventional wisdom they should not occur, such as ca. 1000 Ma (Tonian) ice rafted debris in Scotland (Hartley et al., 2020). In south China, presence of dropstones in the Doushanto Formation cap carbonate has been suggested but not fully described (Huang et al., 2016). Cap carbonate dololaminite facies are often viewed as condensed sedimentation deposits (Kennedy and Christie-Blick, 2011; Rooney et al., 2020). In the Amadeus Basin, Australia, they may represent basinal facies which by comparison to other cap dolostones may represent tens of millions of years (Kennedy and Christie-Blick, 2011). Whilst rates of deposition of the cap dolostones are unknown, consideration of Cryogenian glacial successions that underlie such sequences point to extremely low rates of accumulation by comparison to Phanerozoic glaciations (Partin and Sadler, 2016), which would also be consistent with a “condensed” origin for the glacial facies (Kennedy and Christie-Blick, 2011). If the Rasthof dololaminites do represent many millions of years deposition, then they testify to the operation of ice-rafting processes over a similar time interval.

The juxtaposition of what have traditionally been regarded as warm water cap carbonates immediately overlying cold climate diamictites is an intriguing paradox of the Cryogenian icehouse.

The boundary between the two has been recognised and correlated worldwide and used to attest to globally synchronous terminal deglaciation at least twice during the Neoproterozoic, with cap carbonates viewed as isochronous (e.g. Rooney et al., 2020; Yu et al., 2020). The presence of recurring dropstone horizons in one of the iconic cap carbonates casts suggests that existing models must be reappraised to incorporate the presence of ice during deposition. It further questions the chronostratigraphic significance of these deposits as the definitive marker of the end of Cryogenian glaciation in one locality, inviting a careful reconsideration of their significance on a global scale.

Acknowledgments

We are grateful to Max Lechte, to two anonymous reviewers, and the input of the editor William Clyde whose suggestions on an earlier version of the paper improved the manuscript greatly.

REFERENCES CITED

Bechstädt, T., Jäger, H., Rittersbacher, A., Schweisfurth, B., Spence, G., Werner, G., and Boni, M., 2018, The Cryogenian Ghaub Formation of Namibia – New insights into Neoproterozoic glaciations: Earth-Science Reviews, v. 177, p. 678–714. https://doi.org/10.1016/j.earscirev.2017.11.028

Bennett, M. R., Doyle, P., and Mather, A. E., 1996, Dropstones: Their origin and significance: Palaeogeography, Palaeoclimatology, Palaeoecology, v. 121, p. 331–339. https://doi.org/10.1016/0031-0182(95)00071-2

Bosak, T., Lahr, J.G., Pruss, S.B., MacDonald, F.A., Gooday, A.J., Dalton, L., and Matys, E.D., 2012, Possible early foraminiferans in post-Sturtian (713–636 Ma) cap carbonates: Geology, v. 40, p. 67–70.

Busfield, M. E., and Le Heron, D. P., 2013, Glacitectonic deformation in the Chuos formation of northern Namibia: Implications for Neoproterozoic ice dynamics: Proceedings of the Geologists' Association, v. 124. https://doi.org/10.1016/j.pgeola.2012.10.005

Busfield, M. E., and Le Heron, D. P., 2018, Snowball earth under the microscope: Journal of Sedimentary Research, v. 88. https://doi.org/10.2110/jsr.2018.34

Chewings, J. M., Atkins, C. B., Dunbar, G. B., and Golledge, N. R., 2014, Aeolian sediment transport and deposition in a modern high-latitude glacial marine environment: Sedimentology, 61, p. 1535–1557. https://doi.org/10.1111/sed.12108

Dalton, L.A., Bosak, T., Macdonald, F.A., Lahr, D.J.G., and Pruss, S.B., 2013, Preservational and morphological variability of assemblages of agglutinated eukaryotes in Cryogenian cap carbonates of northern Namibia: Palaios, v. 28, p. 67–79.

Del Cortona, A., Jackson, C. J., Bucchini, F., Van Bel, M., D'hondt, S., Skaloud, P., Delwiche, C. F., Knoll, A. H., Raven, J. A., Verbruggen, H., Vandepoele, K., De Clerck, O., and Leliaert, F., 2020, Neoproterozoic origin and multiple transitions to macroscopic growth in green seaweeds: Proceedings of the National Academy of Sciences of the United States of America, v. 117, p. 2551–2559. https://doi.org/10.1073/pnas.1910060117

Eyles, N. and Januszczak, N., 2007, Syntectonic subaqueous mass flows of the Neoproterozoic Otavi Group, Namibia: where is the evidence of global glaciation? Basin Research, v. 19, p. 179–198.

Fabre, S., and Berger, G., 2012, How tillite weathering during the snowball Earth aftermath induced cap carbonate deposition: Geology, v. 40, p. 1027–1030. https://doi.org/10.1130/G33340.1

Fairchild, I.J., Hambrey, M.J., Spiro, B., and Jefferson, T.H., 1989, Late Proterozoic glacial carbonates in northeast Spitsbergen: new insights into the carbonate-tillite association: Geological Magazine, v. 126, p. 469-490.

Hartley, A., Kurjanski, B., Pugsley, J., and Armstrong, J., 2019, Ice-rafting in lakes in the early Neoproterozoic: dropstones in the Diabaig Formation, Torridon Group, NW Scotland: Scottish Journal of Geology, https://doi.org/10.1144/sjg2019-017

Hodell, D. A., Nicholl, J. A., Bontognali, T. R. R., Danino, S., Dorador, J., Dowdeswell, J. A., Einsle, J., Kuhlmann, H., Martrat, B., Mleneck-Vautravers, M. J., Rodríguez-Tovar, F. J., and Röhl, U., 2017, Anatomy of Heinrich Layer 1 and its role in the last deglaciation: Paleoceanography, v. 32, p. 284–303. https://doi.org/10.1002/2016PA003028

Hoffman, P. F., and Schrag, D. P., 2002, The snowball Earth hypothesis: Testing the limits of global change: Terra Nova, v. 14, p. 129–155. https://doi.org/10.1046/j.1365-3121.2002.00408.x

Hoffman, P.F. and Halverson, G.P., 2008, Otavi Group of the western Northern Platform, the eastern Kaoko Zone and the western Northern Margin Zone: In: The Geology of Namibia Volume 2 – Neoproterozoic to Lower Palaeozoic (Ed. R. McG Miller), pp. 13.69–13.136. Ministry of Mines and Energy, Windhoek, Namibia.

Hoffman, P. F., Kaufman, A. J., Halverson, G. P., and Schrag, D. P., 1998, A Neoproterozoic snowball Earth: Science, v. 281, p. 1–5. https://doi.org/10.1126/science.281.5381.1342

Hoffman, P. F., Lamothe, K. G., LoBianco, S. J. C., Hodgskiss, M. S. W., Bellefroid, E. J., Johnson, B. W., Hodgin, E. B., and Halverson, G. P., 2017, Sedimentary depocenters on Snowball Earth: Case studies from the Sturtian Chuos formation in Northern Namibia: Geosphere, v. 13, p. 811–837. https://doi.org/10.1130/GES01457.1

Huang, K. J., Teng, F. Z., Shen, B., Xiao, S., Lang, X., Ma, H. R., Fu, Y., and Peng, Y., 2016, Episode of intense chemical weathering during the termination of the 635 Ma Marinoan glaciation: Proceedings of the National Academy of Sciences of the United States of America, v. 113, p. 14904–14909. https://doi.org/10.1073/pnas.1607712113

Kennedy, K. and Eyles, N., 2020, Syn-rift mass flow generated 'tectonofacies' and 'tectonosequences' of the Kingston Peak Formation, Death Valley, California, and their bearing on supposed Neoproterozoic panglacial climates: Sedimentology, https://doi.org/10.1111/sed.12781

Kennedy, M. J., and Christie-Blick, N., 2011, Condensation origin for Neoproterozoic cap carbonates during deglaciation: Geology, v. 39, p. 319–322. https://doi.org/10.1130/G31348.1

Kennedy, M. J., Christie-Blick, N., and Sohl, L. E., 2001, Are Proterozoic cap carbonates and isotopic excursions a record of gas hydrate destabilization following Earth's coldest intervals? Geology, v. 29, p. 443–446. https://doi.org/10.1130/0091-7613(2001)029<0443:APCCAI>2.0.CO;2

Lamb, M. P., Fischer, W. W., Raub, T. D., Taylor Perron, J., and Myrow, P. M., 2012, Origin of giant wave ripples in snowball earth cap carbonate: Geology, v. 40, p. 827–830. https://doi.org/10.1130/G33093.1

Le Ber, E., Le Heron, D. P., Winterleitner, G., Bosence, D. W. J., Vining, B. A., and Kamona, F., 2013, Microbialite recovery in the aftermath of the Sturtian glaciation: Insights from the Rasthof Formation, Namibia: Sedimentary Geology, v. 294, p. 1–12. https://doi.org/10.1016/j.sedgeo.2013.05.003

Le Heron, D. P., Busfield, M. E., and Kamona, F., 2013, An interglacial on snowball Earth? Dynamic ice behaviour revealed in the Chuos Formation, Namibia: Sedimentology, v. 60, p. 411–427. https://doi.org/10.1111/j.1365-3091.2012.01346.x

Oviatt, C. G. J., 2019, Geomorphic controls on sedimentation in Pleistocene Lake Bonneville, eastern Great Basin. From Saline to Freshwater: The Diversity of Western Lakes in Space and Time, 2536(04), 53–66. https://doi.org/10.1130/2018.2536(04)

Partin, C.A., and Sadler, P.M., 2016, Slow net sediment accumulation sets snowball Earth apart from all younger glacial episodes: Geology 44, 1019-1022.

Peakall, J., Best, J., Baas, J.H., Hodgson, D.M., Clare, M.A., Talling, P.J., Dorrell, R.M., Lee, D.R., 2020, An integrated process-based model of flutes and tool marks in deep-water environments: Implications for palaeohydraulics, the Bouma sequence and hybrid event beds: Sedimentology, v. 67, p. 1601–1666. https://doi.org/10.1111/sed.12727

Rodríguez-López, J. P., Liesa, C. L., Pardo, G., Meléndez, N., Soria, A. R., and Skilling, I., 2016, Glacial dropstones in the western Tethys during the late Aptian-early Albian cold snap: Palaeoclimate and palaeogeographic implications for the mid-Cretaceous. Palaeogeography, Palaeoclimatology, Palaeoecology: v. 452, p. 11–27. https://doi.org/10.1016/j.palaeo.2016.04.004

Rooney, A.D., Yang, C., Condon, D.J., Zhu, M., Macdonald, F.A., 2020, U-Pb and Re-Os geochronology tracks stratigraphic condensation in the Sturtian snowball Earth aftermath: Geology, v. 48, p. 625–629. https://doi.org/10.1130/G47246.1

Shields, G. A., 2005, Neoproterozoic cap carbonates: A critical appraisal of existing models and the plumeworld hypothesis: Terra Nova, v. 17, p. 299–310. https://doi.org/10.1111/j.1365-3121.2005.00638.x

Tomkins, J.D., Lamoureux, S.F., Antoniades, D., Vincent, W.F., 2008, Sedimentary pellets as an ice-cover proxy in a High Arctic ice-covered lake: Journal of Paleolimnology, v. 41, p. 225-242. https://doi.org/10.1007/s10933-008-9255-x

Vesely, F. F., and Assine, M. L., 2014, Ice-Keel Scour Marks In the Geological Record: Evidence From Carboniferous Soft-Sediment Striated Surfaces In the Parana Basin, Southern Brazil: Journal of Sedimentary Research, v. 84, p. 26–39. https://doi.org/10.2110/jsr.2014.4

Yan, B., Shen, W., Zhao, N., and Zhu, X., 2020, Constraints on the nature of the Marinoan glaciation: Cyclic sedimentary records from the Nantuo Formation, South China: Journal of Asian Earth Sciences, v. 189, 104137. https://doi.org/10.1016/j.jseaes.2019.104137

Yu, W., Algeo, T.J., Zhou, Q., Du, Y., Wang, P. 2020. Cryogenian cap carbonate models: a review and critical assessment. Palaeogeography, Palaeoclimatology, Palaeoecology, 552, 109727.

Zalasiewicz, J., and Taylor, L., 2001, Deep-basin dropstones in the early Silurian of Wales: A clue to penecontemporaneous, near-shore algal forests: Proceedings of the Geologists' Association, v. 112, p. 63–66. https://doi.org/10.1016/S0016-7878(01)80050-X

Figure captions

Figure 1: Geotectonic map of northern Namibia (after Hoffman and Halverson, 2008), showing the location of the two study areas at Omutirapo (19° 6.999'S, 13° 56.170'E) and Rasthof Farm (19° 20.004'S, 14° 44.272'E).

Figure 2: A. Stratigraphy of the Otavi Group. The maximum age constraint for the Chuos, 747 ± 2Ma, is based on U-Pb dating of Askevold Formation volcanics in the Ombombo Subgroup (Hoffmann et al., 2004). The upper glacial unit, the Ghaub, exhibits a 635 ± 1Ma depositional age from U-Pb dating of ash beds (Hoffman et al., 1996). B: Summary sedimentary logs of the uppermost part of the Chuos Formation (base not shown) and the lower part of the Rasthof Formation at both Omutirapo and Rasthof Farm.

Figure 3: Stratigraphic relationships and lonestone-bearing strata at Omutirapo. A: Stratigraphic contact between sheared diamictites of the Chuos Formation (below the hammer) and dololaminites of the basal Rasthof Formation (above the hammer). B: a tripartite interval consisting of dololaminites at the base, normally graded packstone-grainstone in the middle, and dololaminites at the top. C: ca. 1 m thick floatstone interval sandwiched between dololaminites. This floatstone interval is the lateral equivalent of the normally graded packstone-grainstone shown in B. D: Detail of the floatstone bed with sub-rounded to rounded clasts. E: Sheared and attenuated clasts at the bottom of the floatstone interval in C (next to the head of the hammer).

Figure 4: Outcrop view of the section at Rasthof Farm, showing vertically inclined strata that young to the left. The position of the profile in Fig. 2 is shown, as it the location of the lonestone-bearing strata in the Rasthof Formation. A: Dololaminites with abundant lonestones, many of which show evidence for impact structures, punctured underlying laminations and undisturbed, draping laminations. Note also the presence of a “clast cluster” at the bottom right hand corner of the image. Evidence for normal faults with mm-scale offset, capped by undisturbed laminations, is seen throughout the section. C and D: Quartz granule in disturbed laminations; note also the presence of pyrite (Pyr) throughout. E: Two examples of completely isolated lonestones within the dololaminites, each showing impact structures. F: Thin section image. Upper part is largely undeformed, with evidence for impact structures beneath lonestones and undisturbed, draping laminations. The bottom part of the image shows multiple lines of evidence for soft-sediment deformation, including a normal fault and intralamina folds. These features are interpreted as the products of early compaction.

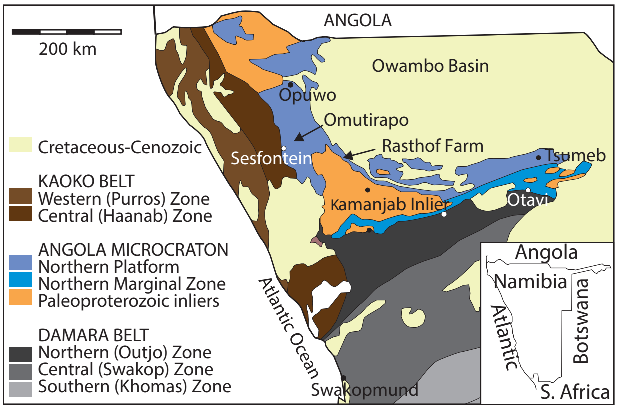

ANGOLA
200 km
Owambo Basin
Opuwo
Omutirapo
Rasthof Farm
Sesfontein
Tsumeb
Kamanjab Inlier
Otavi
Atlantic Ocean
Swakopmund
Cretaceous-Cenozoic
KAOKO BELT
Western (Purros) Zone
Central (Haanab) Zone
ANGOLA MICROCRATON
Northern Platform
Northern Marginal Zone
Paleoproterozoic inliers
DAMARA BELT
Northern (Outjo) Zone
Central (Swakop) Zone
Southern (Khomas) Zone
Angola
Namibia
Atlantic
Botswana
S. Africa

Fig. 1

Fig. 2

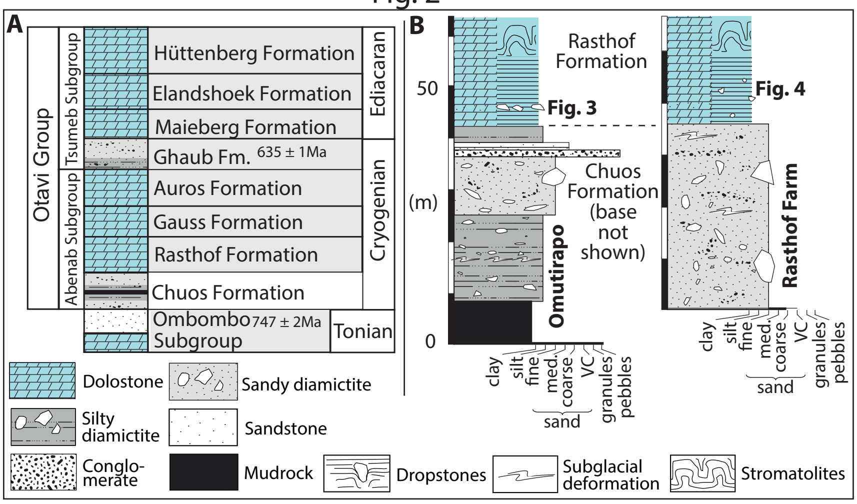

A
Otavi Group
Tsumeb Subgroup
Abenab Subgroup
Hüttenberg Formation
Elandshoek Formation
Maieberg Formation
Ghaub Fm. 635 ± 1Ma
Auros Formation
Gauss Formation
Rasthof Formation
Chuos Formation
Ombombo 747 ± 2Ma
Subgroup
Ediacaran
Cryogenian
Tonian
B
50
(m)
0
Rasthof
Formation
Fig. 3
Chuos
Formation
(base
not
shown)
Omutirapo
Fig. 4
Rasthof Farm
clay
silt
fine
med.
coarse
VC
granules
pebbles
sand
Dolostone
Sandy diamictite
Silty
diamictite
Sandstone
Conglo-
merate
Mudrock
Dropstones
Subglacial
deformation
Stromatolites

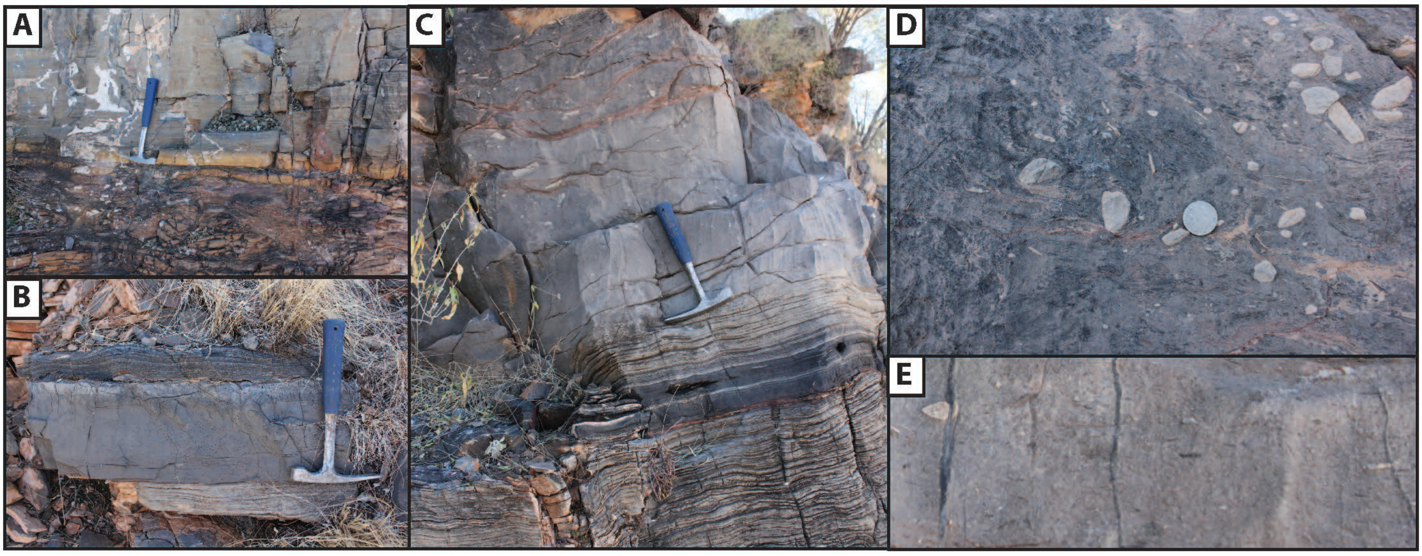

Fig. 3

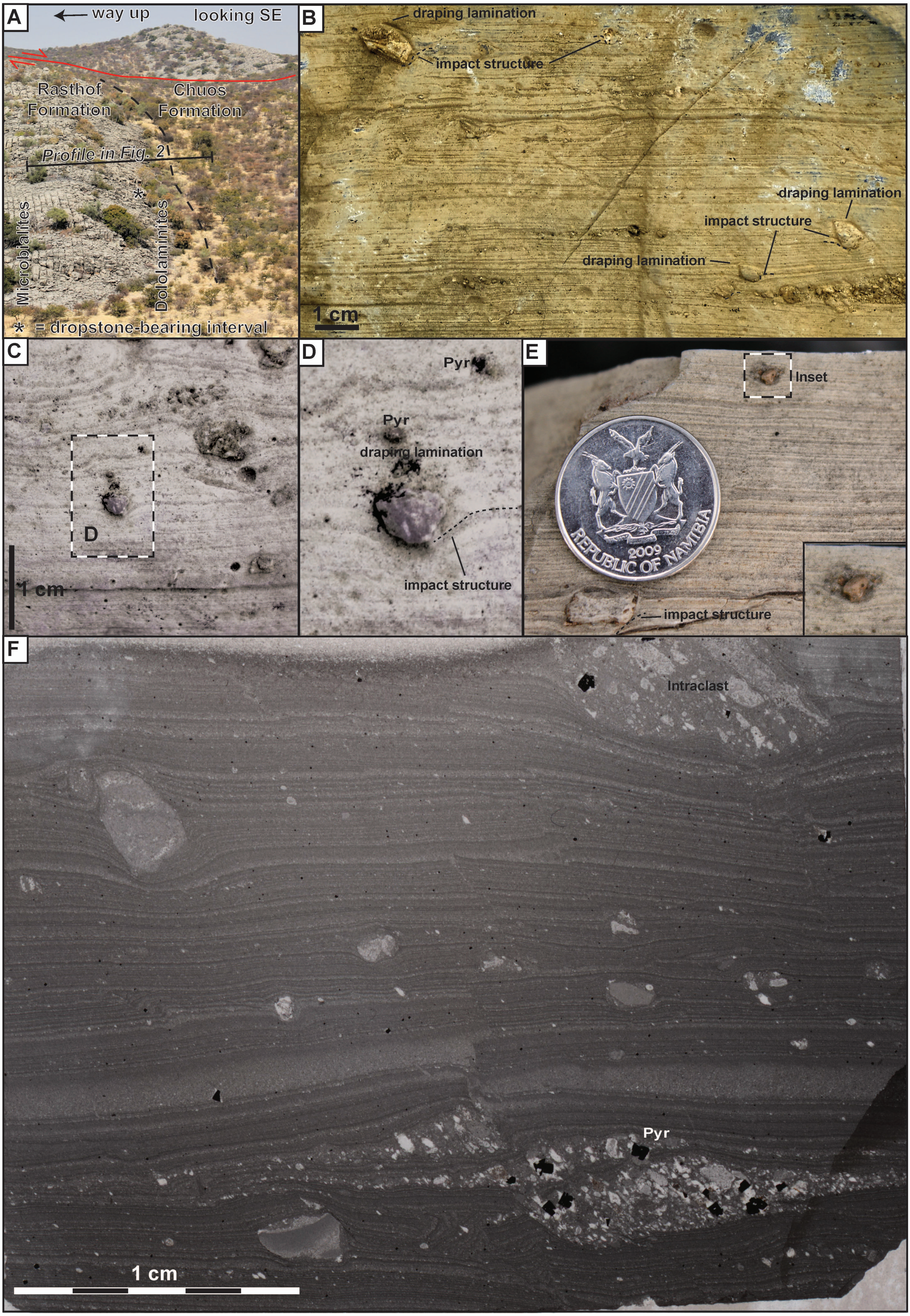
A
way up
looking SE
Rasthof Formation
Chuos Formation
Profile in Fig. 2
Microbialites
Dololaminites
* = dropstone-bearing interval
B
draping lamination
impact structure
draping lamination
impact structure
draping lamination
1 cm
C
D
1 cm
D
Pyr
Pyr
draping lamination
impact structure
E
Inset
2009
REPUBLIC OF NAMIBIA
impact structure
F
Intraclast
Pyr
1 cm

Fig. 4